

1 **Thrombocyte inhibition restores protective immunity to mycobacterial** 2 **infection**

3 Elinor Hortle¹, Khelsey E. Johnson², Matt D. Johansen¹, Tuong Nguyen¹, Jordan A. Shavit³,
4 Warwick J. Britton^{1,4}, David M. Tobin², Stefan H. Oehlers^{1,4} *

5

6 ¹ Tuberculosis Research Program, Centenary Institute, University of Sydney, Camperdown,
7 NSW 2050, Australia

8 ² Department of Molecular Genetics and Microbiology, Duke University School of Medicine,
9 Durham, NC 27710, USA

10 ³ Department of Pediatrics and Cellular and Molecular Biology Program, University of
11 Michigan, Ann Arbor, MI 48107, USA

12 ⁴ Central Clinical School and Marie Bashir Institute, The University of Sydney,
13 Camperdown, NSW 2050, Australia

14 * Corresponding author email: stefan.oehlers@sydney.edu.au, Twitter: @oehlerslab

15

16 **Summary**

17 Infection-induced thrombocytosis is a clinically important complication of tuberculosis
18 infection. Recent studies have highlighted the utility of aspirin as a host-directed therapy
19 modulating the inflammatory response to infection, but have not investigated the possibility
20 that the effect of aspirin is related to an anti-platelet mode of action. Here we utilise the
21 zebrafish-*Mycobacterium marinum* model to show mycobacteria drive host haemostasis
22 through the formation of granulomas. Treatment of infected zebrafish with aspirin markedly
23 reduced mycobacterial burden. This effect is reproduced by treatment with platelet-specific
24 glycoprotein IIb/IIIa inhibitors demonstrating a detrimental role for infection-induced
25 thrombocytosis. We find that the reduction in mycobacterial burden is dependent on

26 macrophages and granuloma formation. Our study identifies haemostasis as a novel virulence
27 mechanism of pathogenic mycobacteria and provides evidence of platelet activation as an
28 efficacious target of aspirin, a widely available and affordable host-directed
29 therapy candidate for tuberculosis.

30

31 **Keywords**

32 Mycobacterial infection, haemostasis, innate immunity, clotting, platelet

33

34 **Introduction**

35 *Mycobacterium tuberculosis* is the world's most lethal pathogen, causing nearly 2 million
36 deaths each year (World Health Organization. and Global Tuberculosis Programme.). The
37 increasing incidence of both multi- and extremely-drug resistant tuberculosis (TB) urgently
38 require the development of therapeutics that overcome the shortcomings of conventional
39 antibiotics. Pathogenic mycobacteria co-opt numerous host pathways to establish persistent
40 infection, and subversion of these interactions with host-directed therapies (HDTs) has been
41 shown to reduce the severity of infection in animal models. For example, we have recently
42 shown that mycobacteria induce host angiogenesis and increase host vascular permeability;
43 blockade of either of these processes reduced both the growth and spread of bacteria (Oehlers
44 et al., 2017; Oehlers et al., 2015). Therefore, host processes co-opted by the bacteria provide
45 attractive targets for novel TB treatments. One such pathway may be haemostasis.

46

47 Thrombocytosis has long been recognised as a biomarker for advanced TB, and infection is
48 often accompanied by the induction of a hypercoagulable state, resulting in increased risk of
49 deep vein thrombosis and stroke (Kutiya et al., 2017; Robson et al., 1996). Recent evidence
50 hints that mycobacteria may drive this process, and that it may aid their growth. For example,

51 cell wall components from *M. tuberculosis* can induce expression of tissue factor - an
52 important activator of coagulation - in macrophages (Kothari et al., 2012). In mice and
53 humans markers of platelet activation are upregulated during *M. tuberculosis* infection (Dong
54 et al., 2018; Fox et al., 2018), and it has been shown *in vitro* that interaction with activated
55 platelets increases the conversion of infected macrophages into cells permissive for bacterial
56 growth (Feng et al., 2014; Fox et al., 2018). To date the pathogenic roles of haemostasis have
57 not been dissected in an intact *in vivo* model of mycobacterial infection.

58

59 Here we used the zebrafish-*M. marinum* model to investigate the role of host thrombocytes in
60 mycobacterial infection. We show evidence that coagulation and thrombocyte activation are
61 both driven by mycobacteria, and that infection-induced activation of thrombocytes
62 compromises protective immunity. However, clot formation itself has no effect on infection
63 suggesting direct communication between the mycobacterial infection milieu and
64 thrombocytes.

65

66 **Results**

67

68 ***Mycobacterium marinum* induces coagulation in zebrafish.**

69

70 To determine if *M. marinum* induces coagulation in zebrafish, we infected *Tg(fabp10a:fgb-*
71 *EGFP)* transgenic embryos expressing EGFP-tagged fibrinogen beta (FGB) with *M.*
72 *marinum*-tdtomato, and imaged the developing infection every 15 minutes from 3 days post
73 infection (DPI), until 6 DPI (Supplementary Video 1). We observed that clots formed only at
74 areas of bacterial growth, and that the size of the clots increased as the number of bacteria
75 increased over the course of the infection (Figure 1A). When we infected fish with Δ ESX1

76 mutant *M. marinum*, which lacks the ability to export key virulence proteins and does not
77 form granulomas, we observed significantly reduced clot formation (Figures 1B-C).
78 Together, these data demonstrate that coagulation is a conserved consequence of infection
79 driven by pathogenic mycobacteria across host species. Treatment with the anti-coagulant
80 warfarin to prevent clot formation during infection did not affect bacterial burden, suggesting
81 coagulation itself does not affect bacterial growth within the host (Figures 1D-E and S1).

82

83 ***Mycobacterium marinum* infection induces thrombocytosis in zebrafish.**

84

85 To determine if *M. marinum* induces thrombocytosis in zebrafish, we infected *Tg(cd41:GFP)*
86 embryos, where thrombocytes are marked by GFP expression, with red fluorescent
87 *M. marinum*. Infected embryos had significantly increased density of thrombocytes around
88 the tail venous plexus where granulomas preferentially form (Figures 1F and S2A-B).
89 Amongst infected embryos, there was a strong positive correlation between thrombocyte
90 density and mycobacterial burden (Figure S2C). This increased thrombocyte density, and the
91 positive correlation between density and burden, were also observed in Δ ESX1 mutant
92 *M. marinum* infection (Figures S2D-E), indicating that mycobacteria-induced thrombocytosis
93 is ESX1 independent.

94

95 Because the *cd41* promoter is active in non-motile thrombocyte precursors within their
96 caudal haematopoietic tissue, we could not conclusively determine if these thrombocytes had
97 actively migrated to and been retained at the site of infection (Lin et al., 2005). To determine
98 if zebrafish thrombocytes are recruited to sites of mycobacterial infection, we performed
99 trunk injection of *M. marinum* in *Tg(cd41:GFP)* at 3 days post fertilization (DPF), a time
100 point after which mature thrombocytes are in the circulation. Embryos were then imaged at 2,

101 3, and 4 DPI. Thrombocytes were co-localised with the sites of infection in 87% of fish.
102 Rather than forming a stable and growing clot over a period of days (as we observed for
103 FGB), thrombocytes appeared to form transient associations with sites of infection (Figures
104 1F and S3). In some instances, new thrombocytes seemed to be retained at sites of infection
105 in different locations each day, and in others, thrombocytes appeared to stay stationary for
106 multiple days (Figures 1F and S3). The size of infection-associated thrombocytes varied
107 greatly, suggesting activation and progressive degranulation or death of thrombocytes at sites
108 of infection. Thrombocytes were most often observed on the edges of granulomas consistent
109 with the location of granuloma-defining macrophages (Cronan et al., 2016). Therefore
110 thrombocyte-granuloma interactions appear to be a conserved feature of mycobacterial
111 infection across species.

112

113 **Anti-platelet drugs reduce mycobacterial burden in zebrafish.**

114

115 It has previously been reported that aspirin has a host-protective effect during TB infection
116 (Kroesen et al., 2018; Mai et al., 2018; Misra et al., 2010; Schoeman et al., 2011). Most of
117 these studies have focused on the fact that aspirin is a broadly acting nonsteroidal anti-
118 inflammatory drug (NSAID) that is known to modulate infection-relevant prostaglandin
119 metabolism (Tobin et al., 2012). However, aspirin is also a widely-used platelet inhibitor, and
120 we theorised this capacity may also play a role in the drug's effectiveness against TB (Mai et
121 al., 2018).

122

123 To test this hypothesis we first confirmed that the host-protective effect of aspirin was seen
124 across species by treating *M. marinum*-infected fish with aspirin by immersion.

125 Mycobacterial burden was reduced by approximately 50% in aspirin-treated embryos (Figure
126 2A).

127

128 To determine if the anti-platelet effects of aspirin treatment contribute to the reduced
129 mycobacterial burden, we treated *M. marinum*-infected fish with the platelet-specific, small
130 molecule Glycoprotein IIb/IIIa inhibitors, tirofiban or eptifibatide. These drugs do not inhibit
131 platelet activation and de-granulation, but rather inhibit activated platelets from binding to
132 one-another, and to monocytes. Treatment with either Glycoprotein IIb/IIIa inhibitor
133 phenocopied aspirin by reducing bacterial burden providing direct evidence of a detrimental
134 role for platelets in the immune response to mycobacterial infection (Figure 2B-C).

135

136 We next examined the cellular target of anti-platelet drugs in our infection system. We
137 performed antibacterial testing of the anti-platelet drugs in axenic cultures of *M. marinum*
138 and did not observe any effect on bacterial growth *in vitro* demonstrating host-dependent
139 activity (Figure 2D).

140

141 The specificity of anti-platelet drugs against mycobacterial infection was tested in acute
142 *Pseudomonas aeruginosa* infection. Treatment of *P. aeruginosa*-infected embryos with either
143 class of anti-platelet drug did not affect survival demonstrating specificity against
144 mycobacterial infection (Figure 2E).

145

146 **The anti-bacterial effect of anti-platelet drugs is thrombocyte dependent.**

147 We next confirmed that anti-platelet drugs inhibit thrombocytes in zebrafish using a tail wound
148 thrombosis assay (Figure S4A). Anti-platelet drugs reduced the number of thrombocytes
149 recruited to tail wound clots demonstrating conservation of cellular target in zebrafish embryos

150 (Figure S4B-C). Of the two Glycoprotein IIb/IIIa inhibitors tirofiban and eptifibatide, tirofiban is
151 the more stable small molecule. Therefore we chose to use tirofiban for inhibition of
152 thrombocytes in all further experiments.

153

154 To determine if zebrafish thrombocytes are the conserved target for tirofiban in the zebrafish-
155 *M. marinum* infection model, we inhibited thrombopoiesis by injection with a morpholino
156 against the thrombopoietin receptor *cmpl* (Lin et al., 2005). Inhibition of thrombopoiesis did
157 not affect the outcome of infection. However, tirofiban treatment failed to reduce bacterial
158 burden in thrombocyte-depleted embryos, demonstrating thrombocytes are the cellular target
159 of this drug in the zebrafish infection model (Figure 3A).

160

161 Tirofiban was designed as a specific inhibitor of Glycoprotein IIb/IIIa in mammals (Peerlinck et
162 al., 1993), but nothing is known about its potential off-target effects in the zebrafish. Therefore,
163 to confirm that disruption of Glycoprotein IIb/IIIa binding alone can reduce bacterial burden, we
164 performed infection experiments in Glycoprotein IIb/IIIa knock-out (KO) transgenic embryos
165 (*itga2b* mutants). The *itga2b*^{sa10134} allele caused a dose-dependent reduction in thrombocytes
166 recruited to tail wound clots (Figure S5A), and KO of *itga2b* significantly reduced bacterial
167 burden (Figure 3B). This demonstrates that inhibition of Glycoprotein IIb/IIIa is sufficient to
168 reduce bacterial burden.

169

170 **Thrombocytes increase mycobacterial burden independently of coagulation.**

171 To assess the contribution of thrombocytes to infection induced coagulation, we analysed the
172 formation of FGB-GFP clots in tirofiban-treated embryos. Tirofiban significantly reduced total
173 clot formation (Figure 3C). However, correction for relative bacterial burden suggested that the

174 reduced clot formation was burden-dependent and thrombus formation was not additionally
175 impacted by tirofiban treatment (Figure 3D).

176

177 Therefore, we hypothesised that tirofiban was reducing bacterial burden independently of
178 infection induced coagulation. To investigate this hypothesis, we again used warfarin, which
179 prevented clot formation during infection and did not affect bacterial burden (Figure 1E). As
180 expected, the addition of warfarin to our tirofiban treatment model had no effect on the ability of
181 tirofiban to reduce bacterial burden (Figure 3E), indicating that tirofiban acts through an
182 independent process. Interestingly, when we addressed the same question using a *fibrinogen*
183 *alpha chain* mutant zebrafish line that does not readily produce clots due to a lack of mature
184 fibrinogen, tirofiban treatment failed to reduce bacterial burden. This suggests that the protective
185 effect of tirofiban occurs independently of fibrin clot formation, but requires the presence of
186 soluble fibrinogen – consistent with the known mechanisms of action for glycoprotein IIb/IIIa
187 inhibitors in mammalian haemostasis (Figure 3F).

188

189 **Thrombocytes compromise immunity through granuloma-associated macrophages.**

190 To further delineate the mechanism by which thrombocytes compromise innate immune control
191 of mycobacterial infection but not the response to *Pseudomonas* infection, we asked if
192 granuloma formation and maturation is essential to pathological thrombocyte activation.

193

194 To examine the requirement of granuloma formation and necrosis for thrombocyte-inhibiting
195 drug efficacy, we infected embryos with Δ ESX1 *M. marinum* that are unable to drive granuloma
196 maturation or necrosis. Tirofiban treatment had no effect on mutant bacterial burden at 5 DPI
197 (Figure 4A). Similarly, in embryos infected with *M. marinum* at a dose too low to form necrotic

198 granulomas by 5 DPI, continuous tirofiban treatment had no effect on bacterial burden at 5 DPI
199 (Figure S6A).

200

201 We next took advantage of the stereotypical progression of innate immune granulomas in
202 zebrafish embryos to investigate the temporal activity of thrombocyte inhibition by tirofiban.

203 We found that at 3 DPI, a time-point with nascent granuloma formation but prior to significant
204 granuloma organisation and necrosis, tirofiban had no effect on bacterial burden (Figure 4B).

205 Conversely, treatment of infection from 4 to 5 DPI, a time-point when granulomas are organised
206 and start to become necrotic, tirofiban significantly reduced bacterial burden within 24 hours
207 (Figure 4C).

208

209 Macrophages are key cells in the innate granuloma, therefore to determine if thrombocyte
210 inhibition exerts a protective effect through boosting macrophage-dependent immunity, we to
211 depleted macrophages. We injected clodronate liposomes to deplete macrophages early during
212 granuloma formation at 3 DPI (Figure S6B-C). Anti-platelet drug treatment was started
213 immediately after liposome injection. In macrophage-depleted fish tirofiban did not reduce
214 bacterial burden (Figure 4D), suggesting that thrombocytes promote bacterial growth via
215 macrophages. We also observed that macrophage depletion reduced infection induced
216 thrombocytosis, but did not affect clot formation (Figure S6D-E), again supporting the
217 hypothesis that these two processes operate independently in mycobacterial infection.

218

219 It has previously been shown that in the presence of mycobacteria *in vitro*, platelets
220 accelerate the conversion of macrophages to foam cells, which are permissive for
221 mycobacterial growth, suggesting a mechanism for infection-induced thrombocytosis to
222 compromise innate immunity to mycobacterial infection (Feng et al., 2014). We therefore

223 hypothesised that thrombocyte inhibition would reduce the conversion of macrophages into
224 foam cells. We investigated this by performing Oil-red O staining to measure lipid
225 accumulation within individual granulomas (Figure 4E). Because tirofiban treatment reduced
226 bacterial burden, Oil-red O density was only compared between size-matched granulomas in
227 treatment group. Tirofiban-treated embryos had significantly less Oil-red O accumulation in
228 their granulomas when compared to DMSO control, even after correction for reduced
229 bacterial burden (Figure 4F). Together, these data demonstrate an *in vivo* effect of
230 thrombocyte activation inhibiting an effective immune response by converting macrophages
231 into foam cells in mycobacterial granuloma.

232

233 Given that foam cell formation is closely associated with necrosis in tuberculosis (Russell et
234 al., 2009) we hypothesised that tirofiban treatment would reduce cell death within the
235 granuloma. We therefore used TUNEL staining to detect the fragmented DNA of dying cells
236 in *M. marinum* infected embryos. At 5 DPI, tirofiban-treated embryos showed significantly
237 less TUNEL staining, indicating significantly reduced cell death within the granuloma
238 (Figures 4G-H). Together these results indicate that infection-induced platelet activation
239 aggravates a basal rate of macrophage cell death in the granuloma.

240

241 **Discussion**

242

243 Here we have used the zebrafish-*M. marinum* model to identify infection-induced
244 haemostasis as a detrimental host response that is co-opted by pathogenic mycobacteria. Our
245 data builds on previous studies that have shown coagulation, thrombocytosis and
246 thrombocyte activation are associated with mycobacterial infection, and provides *in vivo*
247 evidence of a direct role for thrombocyte activation in promoting mycobacterial growth. We

248 have shown that infection-induced haemostasis is conserved in the zebrafish-*M. marinum*
249 infection model, and that the platelet inhibiting drugs, aspirin, tirofiban, and eptifibatide, are
250 able to reduce bacterial burden, independently of effects on coagulation, through host-
251 mediated effects.

252

253 A number of studies have investigated aspirin as a possible adjunctive treatment for TB in a
254 range of animal models and human trials (Byrne et al., 2007a, b; Kroesen et al., 2018; Mai et
255 al., 2018; Misra et al., 2010; Schoeman et al., 2011; Tobin et al., 2012). The results of these
256 studies have been far from conclusive, while most found beneficial effects (Byrne et al.,
257 2007a; Kroesen et al., 2018; Mai et al., 2018; Misra et al., 2010; Tobin et al., 2012), one
258 human trial observed no effect (Schoeman et al., 2011), and one mouse study found an
259 antagonistic relationship between aspirin and the frontline anti-tubercular drug isoniazid
260 (Byrne et al., 2007b). This lack of consensus may be due to the fact that the NSAID effect of
261 aspirin will affect many cell types and processes important in the heterogeneous host
262 response to mycobacterial infection. Our study expands this literature by clearly delineating a
263 role for thrombocytosis in compromising the host response to infection using thrombocyte-
264 specific reagents.

265

266 Our study found that coagulation and thrombocytes have distinct roles during the
267 pathogenesis of mycobacterial infection of zebrafish. Inhibiting coagulation alone did not
268 significantly reduce bacterial burden, and therefore we considered anti-platelet treatment as a
269 more attractive HDT than anti-coagulant treatment. Although we found lower total clot
270 formation in tirofiban-treated embryos, this was only proportional to bacterial load, suggesting
271 infection-induced coagulation could be independent of infection-induced thrombocyte
272 aggregation. It must be noted that we only measure a simple single end-point in our zebrafish

273 embryo experiments (bacterial load) at a relatively early time point for a chronic infection. In
274 more complex animals, where stroke and DVT are important secondary complications of
275 mycobacterial infection, reducing coagulation may yet prove to be efficacious as a HDT during
276 TB therapy to reduce morbidity. Conversely, data from the mouse model of TB suggests tissue
277 factor-induced fibrin is necessary to contain mycobacteria within granulomas
278 (Venkatasubramanian et al., 2016).

279

280 Our study provides evidence that infection-induced thrombocytosis is a conserved function of
281 the core mycobacterial pathogenicity program centred around granuloma formation. Our
282 experiments with Δ ESX1 mutant *M. marinum*, which cannot secrete key virulence proteins
283 that drive granuloma formation, demonstrated ESX1-dependent responsiveness to growth
284 restriction by platelet inhibiting drugs. These data fit well with our observations that
285 stationary thrombocytes were only observed around well-developed mycobacterial
286 granulomas, and platelet inhibition was only effective at reducing bacterial burden after the
287 development of significant granuloma pathology. Together these results point to a
288 bidirectional relationship between thrombocyte activation and granuloma maturation.

289

290 Recent research has highlighted the important role of platelets as innate immune cells; they
291 are able to release anti-microbial peptides, pick up and 'bundle' bacteria, and initiate the
292 recruitment of other innate immune cells to sites of infection (Gaertner et al., 2017; Li et al.,
293 2017; Morrell et al., 2014). The low frequency at which direct thrombocyte-mycobacterial
294 interactions were observed in our study argues against thrombocytes having a significant role in
295 directly mediating immunity to mycobacterial infection. However, it has been shown that
296 activated platelets can form complexes with monocytes and neutrophils through fibrinogen
297 binding to glycoprotein IIb/IIIa, and that this alters immune cell function (Kral et al., 2016;

298 Sanderson et al., 1998; Weber and Springer, 1997). Moreover, patients with pulmonary
299 tuberculosis have been shown to have significantly increased platelet-monocyte aggregation
300 (Kullaya et al., 2018). It is therefore possible that tirofiban is working in our model by blocking
301 thrombocyte-monocyte aggregation. This hypothesis is supported by our data showing that
302 tirofiban does not reduce bacterial burden in either fibrinogen alpha knock-out fish or in
303 macrophage depleted fish.

304

305 Our experiments demonstrating macrophage-dependence for anti-platelet drug mediated control
306 of infection and reduced lipid accumulation in the granuloma suggest that infection-induced
307 thrombocyte activation modulates macrophage containment of infection. Our study joins
308 several *in vitro* studies that have shown platelets can induce macrophages to have differential
309 responses to bacteria or other pathologic stimuli. In the presence of *S. aureus*, thrombin-
310 activated platelets induce macrophages to increase phagocytosis and slow the growth of
311 bacteria (Ali et al., 2017). Conversely, platelets can suppress the macrophage response to LPS
312 (Ando et al., 2016), and induce macrophages to produce less TNF, more IL-10, and less IL-
313 1 β in response to both BCG and *M. tuberculosis* (Feng et al., 2014; Fox et al., 2018; Kullaya
314 et al., 2018). Crucially it has been shown that platelets are necessary for the formation of
315 foam cells in the context of mycobacterial infection and atheroma (Feng et al., 2014). Our
316 experiments with both Oil Red O and TUNEL staining demonstrate that thrombocytes induce
317 similar pathways *in vivo* in response to *M. marinum*; directing macrophages towards foam-
318 cell formation and necrosis.

319

320 Here we used the zebrafish-*M. marinum* model to show that mycobacteria drive coagulation
321 and thrombocytosis through the formation of granulomas. We found that inhibition of
322 thrombocyte activation was able to reduce foam-cell formation and cell death within the

323 granuloma, leading to dramatically reduced bacterial burden. This is the first *in*
324 *vivo* experimental evidence that infection-induced platelet activation contributes to the
325 pathogenesis of mycobacterial infection. Our study identifies platelet activation as a potential
326 target for tuberculosis host-directed therapy.

327

328 **Acknowledgements**

329 We thank Dr Kristina Jahn and Sydney Cytometry for assistance with imaging equipment;
330 Garvan Biological Testing Facility staff Ms Jennifer Brand, Mr Michael Pickering, Ms Rola
331 Bazzi, Dr Lucie Nedved and Dr Stephanie Allison at the Garvan Institute of Medical
332 Research for maintenance of zebrafish breeding stock; and Professors Lalita Ramakrishnan,
333 Shaun Jackson and Georges Grau, Associate Professor Carl Feng and Dr Jorn Coers for
334 helpful discussion of results.

335

336 This work was supported by the Australian National Health and Medical Research Council
337 APP1099912 and APP1053407; University of Sydney Fellowship; NSW Ministry of Health
338 under the NSW Health Early-Mid Career Fellowships Scheme; and the Kenyon Family
339 Foundation Inflammation Award (S.H.O.), Duke Summer Research Opportunities Program
340 (K.J.), NIH Director's New Innovator Award 1DP2-OD008614 (D.M.T), NIH R01-
341 HL124232 and R01-HL125774 (J.A.S.).

342

343 **Author contributions**

344 E.H., D.M.T. and S.H.O designed the experiments. E.H., K.E.J., M.D.J., T.N. and S.H.O
345 performed the experiments. J.A.S. generated transgenic and mutant zebrafish lines. E.H. and
346 S.O. wrote the paper. W.J.B., D.M.T. and S.H.O. supervised the project.

347

348 **Declaration of Interests**

349 The authors declare no competing interests.

350

351 **References**

352 Ali, R.A., Wuescher, L.M., Dona, K.R., and Worth, R.G. (2017). Platelets Mediate Host

353 Defense against *Staphylococcus aureus* through Direct Bactericidal Activity and by

354 Enhancing Macrophage Activities. *J Immunol* 198, 344-351.

355 Ando, Y., Oku, T., and Tsuji, T. (2016). Platelets attenuate production of cytokines and nitric

356 oxide by macrophages in response to bacterial endotoxin. *Platelets* 27, 344-350.

357 Byrne, S.T., Denkin, S.M., and Zhang, Y. (2007a). Aspirin and ibuprofen enhance

358 pyrazinamide treatment of murine tuberculosis. *The Journal of antimicrobial chemotherapy*

359 59, 313-316.

360 Byrne, S.T., Denkin, S.M., and Zhang, Y. (2007b). Aspirin antagonism in isoniazid treatment

361 of tuberculosis in mice. *Antimicrob Agents Chemother* 51, 794-795.

362 Cronan, M.R., Beerman, R.W., Rosenberg, A.F., Saelens, J.W., Johnson, M.G., Oehlers,

363 S.H., Sisk, D.M., Jurcic Smith, K.L., Medvitz, N.A., Miller, S.E., *et al.* (2016). Macrophage

364 Epithelial Reprogramming Underlies Mycobacterial Granuloma Formation and Promotes

365 Infection. *Immunity* 45, 861-876.

366 Dong, Z., Shi, J., Dorhoi, A., Zhang, J., Soodeen-Lalloo, A.K., Tan, W., Yin, H., Sha, W., Li,

367 W., Zheng, R., *et al.* (2018). Hemostasis and Lipoprotein Indices Signify Exacerbated Lung

368 Injury in TB With Diabetes Comorbidity. *Chest* 153, 1187-1200.

369 Feng, Y., Dorhoi, A., Mollenkopf, H.J., Yin, H., Dong, Z., Mao, L., Zhou, J., Bi, A., Weber,

370 S., Maertzdorf, J., *et al.* (2014). Platelets direct monocyte differentiation into epithelioid-like

371 multinucleated giant foam cells with suppressive capacity upon mycobacterial stimulation. *J*

372 *Infect Dis* 210, 1700-1710.

373 Fox, K.A., Kirwan, D.E., Whittington, A.M., Krishnan, N., Robertson, B.D., Gilman, R.H.,
374 Lopez, J.W., Singh, S., Porter, J.C., and Friedland, J.S. (2018). Platelets Regulate Pulmonary
375 Inflammation and Tissue Destruction in Tuberculosis. *Am J Respir Crit Care Med*.
376 Gaertner, F., Ahmad, Z., Rosenberger, G., Fan, S., Nicolai, L., Busch, B., Yavuz, G.,
377 Luckner, M., Ishikawa-Ankerhold, H., Hennel, R., *et al.* (2017). Migrating Platelets Are
378 Mechano-scavengers that Collect and Bundle Bacteria. *Cell* *171*, 1368-1382 e1323.
379 Johansen, M.D., Kasparian, J.A., Hortle, E., Britton, W.J., Purdie, A.C., and Oehlers, S.H.
380 (2018). Mycobacterium marinum infection drives foam cell differentiation in zebrafish
381 infection models. *bioRxiv*.
382 Kothari, H., Rao, L.V., Vankayalapati, R., and Pendurthi, U.R. (2012). Mycobacterium
383 tuberculosis infection and tissue factor expression in macrophages. *PLoS One* *7*, e45700.
384 Kral, J.B., Schrottmaier, W.C., Salzmann, M., and Assinger, A. (2016). Platelet Interaction
385 with Innate Immune Cells. *Transfus Med Hemoth* *43*, 78-88.
386 Kroesen, V.M., Rodriguez-Martinez, P., Garcia, E., Rosales, Y., Diaz, J., Martin-Cespedes,
387 M., Tapia, G., Sarrias, M.R., Cardona, P.J., and Vilaplana, C. (2018). A Beneficial Effect of
388 Low-Dose Aspirin in a Murine Model of Active Tuberculosis. *Front Immunol* *9*, 798.
389 Kullaya, V., van der Ven, A., Mpagama, S., Mmbaga, B.T., de Groot, P., Kibiki, G., and de
390 Mast, Q. (2018). Platelet-monocyte interaction in Mycobacterium tuberculosis infection.
391 *Tuberculosis (Edinb)* *111*, 86-93.
392 Kutiyal, A.S., Gupta, N., Garg, S., and Hira, H.S. (2017). A Study of Haematological and
393 Haemostasis Parameters and Hypercoagulable State in Tuberculosis Patients in Northern
394 India and the Outcome with Anti-Tubercular Therapy. *Journal of clinical and diagnostic*
395 *research : JCDR* *11*, OC09-OC13.
396 Li, J.L., Zarbock, A., and Hidalgo, A. (2017). Platelets as autonomous drones for hemostatic
397 and immune surveillance. *J Exp Med*.

398 Lin, H.F., Traver, D., Zhu, H., Dooley, K., Paw, B.H., Zon, L.I., and Handin, R.I. (2005).
399 Analysis of thrombocyte development in CD41-GFP transgenic zebrafish. *Blood* *106*, 3803-
400 3810.

401 Mai, N.T., Dobbs, N., Phu, N.H., Colas, R.A., Thao, L.T., Thuong, N.T., Nghia, H.D., Hanh,
402 N.H., Hang, N.T., Heemskerk, A.D., *et al.* (2018). A randomised double blind placebo
403 controlled phase 2 trial of adjunctive aspirin for tuberculous meningitis in HIV-uninfected
404 adults. *eLife* *7*.

405 Matty, M.A., Oehlers, S.H., and Tobin, D.M. (2016). Live Imaging of Host-Pathogen
406 Interactions in Zebrafish Larvae. *Methods Mol Biol* *1451*, 207-223.

407 Misra, U.K., Kalita, J., and Nair, P.P. (2010). Role of aspirin in tuberculous meningitis: a
408 randomized open label placebo controlled trial. *Journal of the neurological sciences* *293*, 12-
409 17.

410 Morrell, C.N., Aggrey, A.A., Chapman, L.M., and Modjeski, K.L. (2014). Emerging roles for
411 platelets as immune and inflammatory cells. *Blood* *123*, 2759-2767.

412 Oehlers, S.H., Cronan, M.R., Beerman, R.W., Johnson, M.G., Huang, J., Kontos, C.D., Stout,
413 J.E., and Tobin, D.M. (2017). Infection-induced vascular permeability aids mycobacterial
414 growth. *J Infect Dis* *215*, 813-817.

415 Oehlers, S.H., Cronan, M.R., Scott, N.R., Thomas, M.I., Okuda, K.S., Walton, E.M.,
416 Beerman, R.W., Crosier, P.S., and Tobin, D.M. (2015). Interception of host angiogenic
417 signalling limits mycobacterial growth. *Nature* *517*, 612-615.

418 Passeri, M.J., Cinaroglu, A., Gao, C., and Sadler, K.C. (2009). Hepatic steatosis in response
419 to acute alcohol exposure in zebrafish requires sterol regulatory element binding protein
420 activation. *Hepatology* *49*, 443-452.

421 Peerlinck, K., De Lepeleire, I., Goldberg, M., Farrell, D., Barrett, J., Hand, E., Panebianco,
422 D., Deckmyn, H., Vermylen, J., and Arnout, J. (1993). MK-383 (L-700,462), a selective

423 nonpeptide platelet glycoprotein IIb/IIIa antagonist, is active in man. *Circulation* 88, 1512-
424 1517.

425 Robson, S.C., White, N.W., Aronson, I., Woollgar, R., Goodman, H., and Jacobs, P. (1996).
426 Acute-phase response and the hypercoagulable state in pulmonary tuberculosis. *Br J*
427 *Haematol* 93, 943-949.

428 Russell, D.G., Cardona, P.J., Kim, M.J., Allain, S., and Altare, F. (2009). Foamy
429 macrophages and the progression of the human tuberculosis granuloma. *Nat Immunol* 10,
430 943-948.

431 Sanderson, H.M., Fox, S.C., Robbins, R.A., Losche, W., Spangenberg, P., and Heptinstall, S.
432 (1998). Role of GPIIb-IIIa in platelet-monocyte and platelet-neutrophil conjugate formation
433 in whole blood. *Platelets* 9, 245-250.

434 Schoeman, J.F., Janse van Rensburg, A., Laubscher, J.A., and Springer, P. (2011). The role
435 of aspirin in childhood tuberculous meningitis. *J Child Neurol* 26, 956-962.

436 Tobin, D.M., Roca, F.J., Oh, S.F., McFarland, R., Vickery, T.W., Ray, J.P., Ko, D.C., Zou,
437 Y., Bang, N.D., Chau, T.T., *et al.* (2012). Host genotype-specific therapies can optimize the
438 inflammatory response to mycobacterial infections. *Cell* 148, 434-446.

439 Venkatasubramanian, S., Tripathi, D., Tucker, T., Paidipally, P., Cheekatla, S., Welch, E.,
440 Raghunath, A., Jeffers, A., Tvinnereim, A.R., Schechter, M.E., *et al.* (2016). Tissue factor
441 expression by myeloid cells contributes to protective immune response against
442 *Mycobacterium tuberculosis* infection. *Eur J Immunol* 46, 464-479.

443 Vo, A.H., Swaroop, A., Liu, Y., Norris, Z.G., and Shavit, J.A. (2013). Loss of fibrinogen in
444 zebrafish results in symptoms consistent with human hypofibrinogenemia. *PLoS One* 8,
445 e74682.

446 Walton, E.M., Cronan, M.R., Beerman, R.W., and Tobin, D.M. (2015). The Macrophage-
447 Specific Promoter *mfap4* Allows Live, Long-Term Analysis of Macrophage Behavior during
448 Mycobacterial Infection in Zebrafish. *PLoS One* *10*, e0138949.

449 Weber, C., and Springer, T.A. (1997). Neutrophil accumulation on activated, surface-
450 adherent platelets in flow is mediated by interaction of Mac-1 with fibrinogen bound to
451 α IIb β 3 and stimulated by platelet-activating factor. *J Clin Invest* *100*, 2085-2093.

452 World Health Organization., and Global Tuberculosis Programme. Global tuberculosis
453 control : WHO report. (Geneva, Global Tuberculosis Programme), p. 15 volumes.

454

455 **Figure legends**

456 **Figure 1: *Mycobacterium marinum* induces coagulation and thrombocytosis around sites** 457 **of infection in zebrafish**

458 A) Representative images of a *Tg(fabp10a:fgb-EGFP)* embryo infected with *M.marinum*-
459 tdTomato by caudal vein injection, showing clot formation (green) at sites of infection (red)
460 at 3, 4, and 5 DPI. B) Representative images of 5 DPI *Tg(fabp10a:fgb-EGFP)* embryos
461 infected with *M.marinum*-tdTomato WT and Δ ESX1 *M. marinum*-td-tomato (Δ ESX1)
462 showing clot formation (green) at sites of infection (red). Arrows indicate clotting. C)
463 Quantification of clot formation in burden-matched Δ ESX1 mutant-infected *Tg(fabp10a:fgb*-
464 *EGFP)* embryos normalised to WT *M. marinum* control. Error lines represent mean \pm SEM,
465 statistical analysis by T test. Data show combined results from two independent experiments.
466 D) Representative images of *Tg(fabp10a:fgb-EGFP)* embryos, where clot formation can be
467 visualised by GFP fluorescence, infected with *M.marinum*-tdTomato (red) and treated with
468 either DMSO or warfarin. E) Quantification of clotting in warfarin-treated *Tg(fabp10a:fgb*-
469 *EGFP)* embryos. F) Representative 2 DPI, 3 DPI and 4 DPI images of *Tg(cd41:GFP)* fish
470 infected with *M.marinum*-tdTomato at 3 DPF. White arrow heads show thrombocyte (green)

471 association with areas of bacterial growth (red). Thrombocytes not indicated with an arrow
472 head were circulating and not considered to be associated with bacteria (more detail available
473 in Figure S2C).

474

475 **Figure 2: Anti-platelet drugs reduce bacterial burden in *M. marinum* infection**

476 A) Quantification of bacterial burden in embryos treated with aspirin normalised to DMSO
477 control. Data are combined results of two independent experiments. B) Quantification of
478 bacterial burden in embryos treated with tirofiban normalised to DMSO control. Data are
479 combined results of two independent experiments. C) Quantification of bacterial burden in
480 embryos treated with eptifibatide or DMSO control. D) Quantification of bacterial growth by
481 relative fluorescence in 7H9 broth culture supplemented with drugs as indicated. E) Survival
482 analysis of *P. aerogenosa* PA01 infected embryos treated with anti-platelet drugs as
483 indicated.

484 All graphs show Mean \pm SEM. Statistical analyses performed by T tests and Log-Rank tests
485 where appropriate.

486

487 **Figure 3: The anti-bacterial effect of anti-platelet drugs is thrombocyte dependent**

488 A) Total fluorescence area of *M. marinum* bacteria in larvae injected with either control or
489 cmpl morpholino (MO) to deplete thrombocytes, and then treated with tirofiban (Tiro).
490 Values are normalised to DMSO-treated control MO larvae. Graphs show the combined
491 results of 2 independent experiments. B) Quantification of bacterial burden in in *itga2b*
492 mutant embryos normalised to WT control. Data are combined results of 3 independent
493 experiments. C) Representative images of 5 DPI *Tg(fabp10a:fgb-EGFP)* embryos infected
494 with *M. marinum*-tdTomato and treated with either DMSO or tirofiban. D) Quantification of
495 clotting relative to bacterial burden in embryos treated with tirofiban normalised to DMSO

496 control. Data are combined results of two independent experiments. E) Quantification of
497 bacterial burden in embryos treated with tirofiban, warfarin, or tirofiban and warfarin,
498 normalised to DMSO control. Data are combined results of 2 independent experiments. F)
499 Quantification of bacterial burden in *fga*^{-/-} embryos treated with tirofiban, normalised to
500 *fga*^{+/+} controls. Data are combined results of 2 independent experiments.

501 All graphs show Mean ± SEM. Statistical analyses performed by T tests or ANOVA where
502 appropriate.

503

504 **Figure 4: Thrombocytes compromise immunity through granuloma-associated**
505 **macrophages.**

506 A) Quantification of bacterial burden in embryos infected with Δ ESX1 *M.marinum*-tdTomato
507 and treated with tirofiban. B) Quantification of bacterial burden at 3 DPI after continuous
508 tirofiban treatment from 0 DPI. C) Quantification of bacterial burden at 5 DPI after overnight
509 drug treatment initiated at 4 DPI. D) Quantification of bacterial burden in embryos infected
510 with *M.marinum*-tdTomato, injected with clodronate liposomes and treated with tirofiban
511 from at 3 DPI. E) Representative images of bacterial granulomas chosen for analysis
512 (bacteria are white in greyscale images), and corresponding Oil Red O (ORO) staining (red-
513 brown in color images). F) Quantification of ORO pixel density relative to granuloma
514 bacterial area, in embryos treated with tirofiban, normalised to DMSO control. G)
515 Representative images of bacterial granulomas showing bacteria in red and TUNEL staining
516 in green. F) Quantification of TUNEL positive area within the largest granuloma of
517 individual embryos.

518 All graphs show Mean ± SEM, statistical tests by T-tests. Data are combined results of two
519 independent experiments, except D) and H) which represent single experiments.

520

521

522 **Graphical abstract.**

523 *M. marinum* induces two independent haemostatic processes in the zebrafish: ESX1
524 dependent coagulation (1), and ESX1 independent, macrophage dependent thrombocytosis
525 (2). Bacteria then induce thrombocyte activation - either directly or via the macrophage - (3).
526 Activated thrombocytes, through fibrinogen, are able to bind macrophages and other
527 thrombocytes. These interactions accelerate foam cell formation and macrophage necrosis,
528 promoting bacterial growth (4). Inhibition of thrombocyte fibrinogen binding with anti-
529 platelet drugs like tirofiban, stops these interactions and thereby limits the growth of bacteria.
530 Drugs which reduce coagulation (1) have no effect on bacterial growth.

531

532

533 **Supplementary Figure Legends**

534 **Figure S1**

535 Related to Figure 1. Quantification of clot formation in warfarin-treated embryos infected
536 with *M. marinum*. Error lines represent mean \pm SEM, statistical analysis by T test.

537

538 **Figure S2**

539 Related to Figure 1. A) Representative images of 5 DPI *Tg(cd41:GFP)* embryos infected
540 with *M.marinum*-tdTomato, showing thrombocyte accumulation (green) at sites of bacterial
541 infection (red). B) Quantification of total thrombocyte *Tg(cd41:GFP)* area within the tail of
542 uninfected or WT *M.marinum*-tdTomato infected embryos. C) Correlation between *M.*
543 *marinum* bacterial burden and total thrombocyte *Tg(cd41:GFP)* area within the tail of
544 infected embryos. D) Quantification of total thrombocyte *Tg(cd41:GFP)* area within the tail
545 of uninfected or Δ ESX1 *M.marinum*-tdTomato infected larvae at 5 DPI. E) Correlation

546 between Δ ESX1 *M. marinum* bacterial burden and total thrombocyte *Tg(cd41:GFP)* area
547 within the tail of infected embryos at 5 DPI.

548

549 **Figure S3**

550 Related to Figure 1. Images of 2 DPI, 3 DPI and 4 DPI *Tg(cd41:GFP)* embryos infected with
551 *M.marinum*-tdTomato at 3 DPF. At each time-point, 2 images were taken ~10 seconds apart.
552 Thrombocytes located in the same position in both images were considered stationary (non-
553 circulating), and labelled with a white arrow head.

554

555 **Figure S4**

556 Related to Figure 2. A) Representative images of thrombocyte accumulation at tail wound in
557 4 DPF *Tg(cd41:GFP)* embryos , 4 hours post injury (hpi). B) Quantification of thrombocytes
558 within 100 μ m of the cut site 4 hpi in aspirin-treated embryos. C) Quantification of
559 thrombocytes within 100 μ m of the cut site 4 hpi in tirofiban-treated embryos.

560 Graphs show Mean \pm SEM, statistical testing by T-test.

561

562 **Figure S5**

563 Related to Figure 3. A) Quantification of thrombocytes within 100 μ m of the cut site 4 hours
564 after injury in *itga2b* WT, heterozygous and knock-out embryos.

565

566 **Figure S6**

567 Related to Figure 4. A) Quantification of bacterial burden in embryos infected with a low
568 dose of 10-50 fluorescent *M. marinum* and treated with tirofiban. B) Representative images
569 of caudal haematopoietic tissue in 6 DPF *Tg(mfap4:tdTomato)* embryos, where macrophages
570 are fluorescently labelled, injected with clodronate or PBS liposomes at 4 DPF. C)

571 Quantification of macrophage number by fluorescent pixel count at 5 DPI in embryos
572 injected with clodronate or PBS liposomes at 3 DPI, and treated with tirofiban. D)
573 Quantification of total thrombocyte *Tg(cd41:GFP)* area within the tail of *M.marinum-*
574 *tdTomato* infected embryos injected with clodronate or PBS liposomes at 3 DPI. E)
575 Quantification of clot formation in *M. marinum-tdTomato* infected *Tg(fabp10a:fgb-EGFP)*
576 embryos injected with clodronate or PBS liposomes at 3 DPI. Graphs show Mean \pm SEM,
577 statistical tests by T-tests (A, D, E) or ANOVA (C).

578

579 **Methods**

580 *Zebrafish husbandry*

581 Adult zebrafish were housed at the Garvan Institute of Medical Research Biological Testing
582 Facility (St Vincent's Hospital AWC Approval 1511) and embryos were produced by natural
583 spawning for infection experiments at the Centenary Institute (Sydney Local Health District
584 AWC Approval 2016-022). Zebrafish embryos were obtained by natural spawning and
585 embryos were raised at 28°C in E3 media.

586

587 *Zebrafish lines*

588 Wild type zebrafish are the TAB background. Transgenic lines are: *Tg(fabp10a:fgb-*
589 *EGFP)^{mi4001}* referred to as *Tg(fabp10a:fgb-EGFP)(Vo et al., 2013)*, *Tg(-6.0itga2b:eGFP)^{la2}*
590 referred to as *Tg(cd41:EGFP)(Lin et al., 2005)*, *Tg(mfap4:tdTomato)^{x12}* referred to as
591 *Tg(mfap4:tdTomato)(Walton et al., 2015)*, Mutant allele *fga^{mi}* contains a 26 bp insertion in
592 the *fibrinogen alpha chain* gene (manuscript in preparation).

593

594 *Infection of zebrafish embryos*

595 Aliquots of single cell suspensions of midlog-phase *Mycobacterium marinum* M strain,
596 Δ ESX1 *M. marinum* and *Pseudomonas aeruginosa* PA01 were frozen at -80°C for use in
597 infection experiments. Bacterial aliquots were thawed and diluted with phenol red dye (0.5%
598 w/v). 10-15 nL was injected into the caudal vein or trunk of M-222 (tricaine)-anaesthetised
599 30-48 hpf embryos resulting in a standard infectious dose ~400 fluorescent *M. marinum*.
600 Embryos were recovered into E3 supplemented with 0.036 g/L PTU, housed at 28 °C and
601 imaged on day 5 of infection unless otherwise stated.

602

603 *Drug treatments*

604 Embryos were treated with vehicle control (DMSO or water as appropriate), 10 µg/ml
605 aspirin, 20 µg/ml tirofiban, 10 µM eptifibatide, or 5 µM warfarin. Drugs and E3 were
606 replaced on days 0, 2, and 4 days post infection (DPI) unless otherwise stated.

607

608 *Tail wound thrombosis assay*

609 Three day post fertilisation (DPF) embryos were treated over-night with anti-platelet drugs.
610 They were anaesthetised, and then a small amount of their tail was removed with a scalpel.
611 Embryos were imaged 4 hours post wounding and the number of GFP positive cells within
612 100 µm of the cut site was counted.

613

614 *Imaging*

615 Live zebrafish embryos were anaesthetized in M-222 (Tricaine) and mounted in 3%
616 methylcellulose for imaging on a Leica M205FA or DM6000B fluorescence
617 stereomicroscope. Image analysis was carried out with Image J Software Version 1.51j using
618 fluorescent pixel counts and intensity measurements as previously described (Matty et al.,
619 2016).

620

621 *Axenic culture*

622 A midlog culture of fluorescent *M. marinum* was diluted 1:100 and aliquoted into 96 well
623 plates for drug treatment. Cultures were maintained at 28°C in a static incubator and bacterial
624 fluorescence was measured in a plate reader.

625

626 *Morpholinos:*

627 Embryos were injected at the single cell stage with 1 pmol
628 cMPL (5'-CAGAACTCTCACCCCTTCAATTATAT-3'),
629 or control morpholino (5'-CCTCTTACCTCAGTTACAATTTATA-3').

630

631 *Clodronate liposome injections:*

632 Larvae were injected at 3 DPI (4 DPF) with 10 nl of 5 mg/ml clodronate liposomes or 5
633 mg/ml PBS vehicle liposomes by caudal vein injection.

634

635 *Oil-red O:*

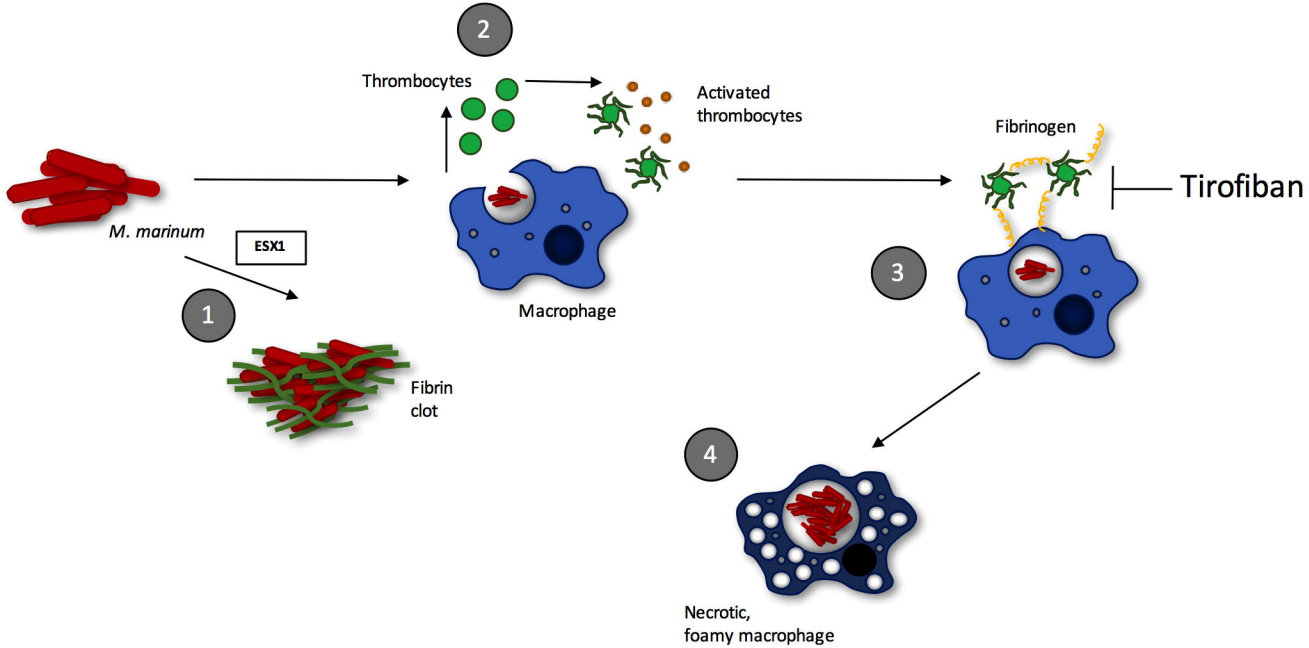
636 Oil Red O lipid staining on whole mount embryos was performed and analysed as previously
637 described (Johansen et al., 2018; Passeri et al., 2009). Briefly, embryos were individually
638 imaged for bacterial distribution by fluorescent microscopy, fixed, and stained in Oil Red O
639 (0.5% w/v in propylene glycol). Oil Red O density was calculated by using the 'measure'
640 function in Image J, and subtracting the mean brightness of a representative region within
641 each granuloma from the mean brightness of a representative adjacent 'background' region.

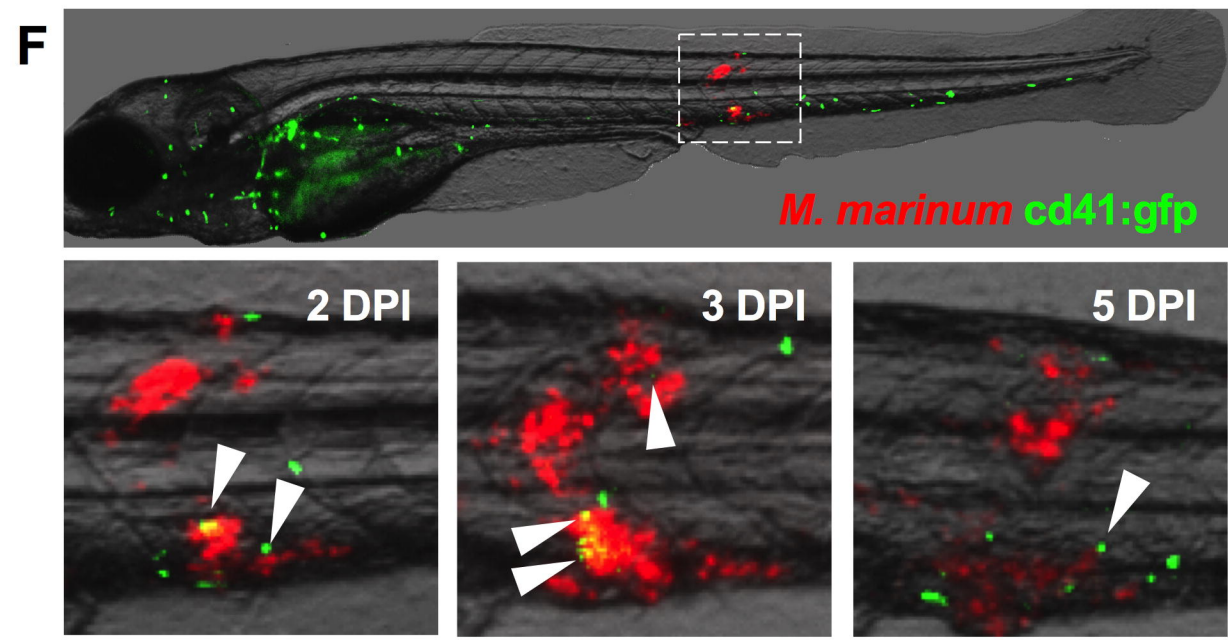
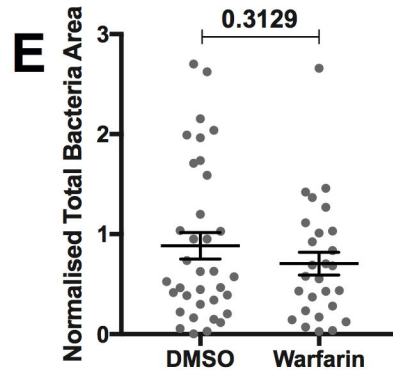
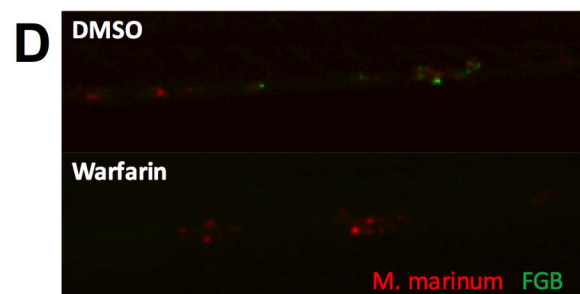
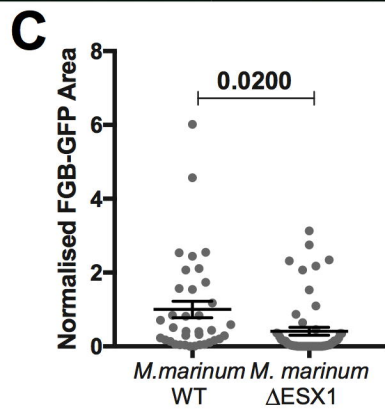
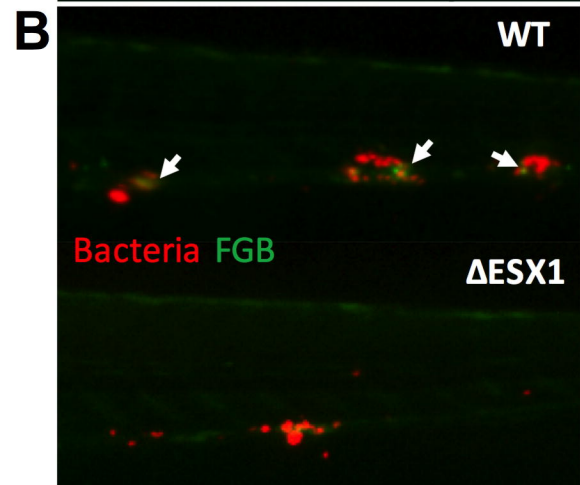
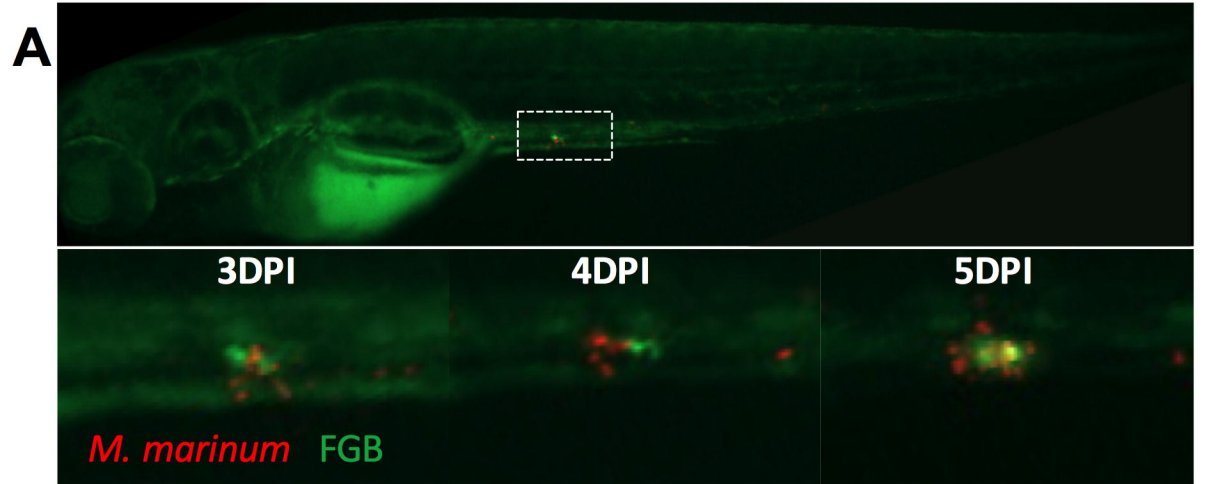
642

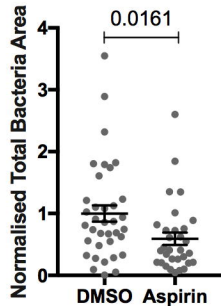
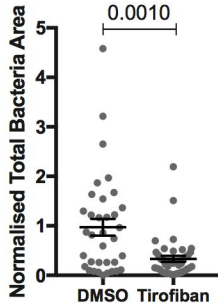
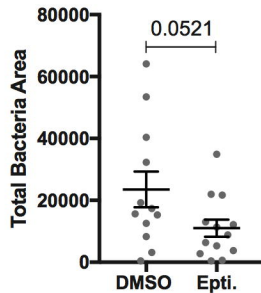
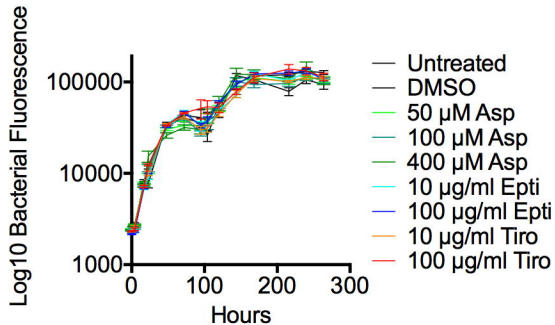
643 *Statistics*

644 All t-tests were unpaired t-tests with Welch's correction. All ANOVA were ordinary one-way
645 ANOVA, comparing the mean of each group with the mean of every other group, using
646 Turkey's multiple comparisons test with a single pooled variance. In cases where data was
647 pooled from multiple experiments, data from each was normalised to its own
648 within-experiment control (usually 'DMSO') before pooling. Outliers were removed using
649 ROUT, with Q=1%.

650





A**B****C****D****E**